# Charcot foot in diabetes and an update on imaging

## Fatma Bilge Ergen, MD[1], Saziye Eser Sanverdi, MD[2]* and Ali Oznur, MD[3]

[1]Department of Radiology, School of Medicine, Hacettepe University, Ankara, Turkey;
[2]Integra Medical imaging Center, Ankara, Turkey; [3]Department of Orthopedics, Ankara Guven Hospital, Ankara, Turkey

Charcot neuroarthropathy (CN) is a serious complication of diabetes mellitus that can cause major morbidity including limb amputation. Since it was first described in 1883, and attributed to diabetes mellitus in 1936, the diagnosis of CN has been very challenging even for the experienced practitioners. Imaging plays a central role in the early and accurate diagnosis of CN, and in distinction of CN from osteomyelitis. Conventional radiography, computed tomography, nuclear medicine scintigraphy, magnetic resonance imaging, and positron emission tomography are the imaging techniques currently in use for the evaluation of CN but modalities other than magnetic resonance imaging appeared to be complementary. This study focuses on imaging findings of acute and chronic neuropathic osteoarthropathy in diabetes and discrimination of infected vs. non-infected neuropathic osteoarthropathy.

*Keywords: diabetes mellitus; complications; diabetic foot; Charcot foot; diagnostic imaging*

Neuropathic arthropathy was first described in 1868 by Jean-Martin Charcot related to tabes dorsalis (1). Although neuropathic osteoarthropathy can be seen in a variety of diseases/conditions other than tabes dorsalis (i.e. leprosy, poliomyelitis, syringomyelia, alcohol abuse, traumatic injury, heavy metal poisoning, multiple sclerosis, congenital neuropathy, and rheumatoid arthritis) today diabetic polyneuropathy is the most common cause of neuropathic osteoarthropathy in developed countries (2–5). After Jordan et al. has first described the association between charcot neuroarthropathy (CN) and diabetes (6) CN has been referred for the specific form of neuropathic arthropathy.

Clinical and radiological diagnosis of CN are both challenging. Clinical presentation of diabetic osteomyelitis and acute CN is similar. Furthermore, osteomyelitis and CN can co-exist in the same extremity. All of these factors pose in a diagnostic dilemma but the imaging plays a pivotal role in arriving at the definitive diagnosis and adequate treatment.

The majority of the patients with CN present between the fifth and sixth decades and most have had diabetes mellitus for a minimum of 10 years. The risk of CN development is not related to the type of diabetes (7). Of all patients with diabetes, 0.1–7.5% have CN and 29% of diabetics with peripheral neuropathy have CN (8, 9). The reported incidence of bilateral involvement varied between 9 and 75% (10, 11). Diabetic CN almost exclusively affects the foot and ankle, other locations being extremely rare (12, 13). It commonly presents in the midfoot, but it may also occur in the forefoot and hindfoot (14).

Diabetic CN has been classified with a variety of classification systems. These systems added the benefit of predicting outcome and prognosis. The most commonly used anatomic system is described by Sanders and Frykberg (15). Pattern 1 involves the phalanges, interphalangeal and the metatarsophalangeal joints; pattern 2 the tarsometatarsal; pattern 3 the cuneonavicular, talonavicular, and calcaneocuboid articulations; pattern 4 the talocrural joint and pattern 5 involves the posterior calcaneus (Fig. 1). Studies have shown that patterns 2 and 3 are the most common, with approximately 45% of cases are pattern 2 and 35% are pattern 3 (16).

Another commonly used classification system is the Brodsky and Rouse system (17). This system describes three anatomic Charcot joints (Types 1, 2, and 3a and 3b): type 1 involves the midfoot; type 2 involves the hindfoot; type 3a involves the ankle; type 3b is a pathologic fracture of the os calcis tubercle. Forefoot CN has a good prognosis whereas hind-foot CN is rare and carries a poor
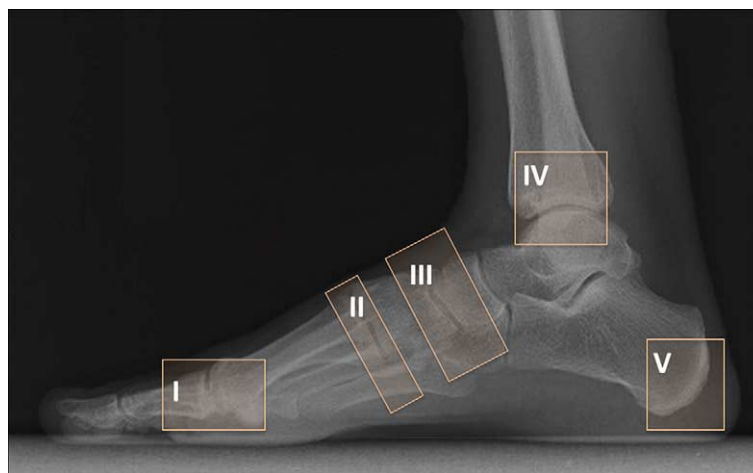
*Fig. 1.* Illustration of Sanders and Frykberg's classification of CN. Pattern I: phalanges, interphalangeal and the metatarsophalangeal joints; pattern II: the tarsometatarsal joints; pattern III: the cuneonavicular, talonavicular, and calcaneocuboid articulations; pattern IV: the talocrural joint; pattern V: the posterior calcaneal involvement.

prognosis due to the effects on weight distribution during walking (9).

This study focuses on imaging findings of acute and chronic neuropathic osteoarthropathy in diabetes and discrimination of infected vs. non-infected neuropathic osteoarthropathy. It also includes the advantages of several imaging modalities to guide the practitioners toward early diagnosis.

## Imaging of acute CN

Acute phase of CN is characterized by a warm, red, and swollen foot and ankle. In a patient with red, hot foot, with no skin ulcers or fever, and a normal or slightly elevated serum C-reactive protein level or erythrocyte sedimentation rate, acute active phase of Charcot process should primarily be considered. However, fever and elevated C-reactive protein or erythrocyte sedimentation rate may also be seen in presence of infection, and in such a condition, the existence of infection cannot be excluded (18).

The tarsal bones and proximal metatarsals, midfoot, are typically affected in the acute stage of the neuropathic osteoarthropathy (18). Involvement of the interphalan-geal joints and ankle is less common (19). The skin temperature of the affected foot is 2–6°C higher than the contralateral foot. Pain may or may not be present, depending on the presence of nerve damage (14, 20). Hyperemia may persist for months or years (21), but in some cases the acute phase rapidly progresses to the chronic stage in days, sometimes less than 6 months, resulting in irreversible deformity (9). The foot is unstable because of collapse of the longitudinal foot arch (22).

Differential diagnosis of the acute CN is infection (i.e. osteomyelitis, cellulitis, septic arthritis, or inflammation (i.e. gout); however, deep vein thrombosis is also a potential mimicker (23).

Plain radiography (PR) is the first choice of imaging in the initial evaluation of CN. The earliest finding of neuroarthic osteoarthropathy in PR is focal demineralization. The flattening of the metatarsal head is often the first sign of diabetic neuroarthropathy. In the absence of soft tissue involvement, subchondral or periarticular changes in the midfoot with polyarticular distribution strongly indicate diabetic neuroarthropathy (24). Subtle changes associated with neuroarthropathy such as occult fractures
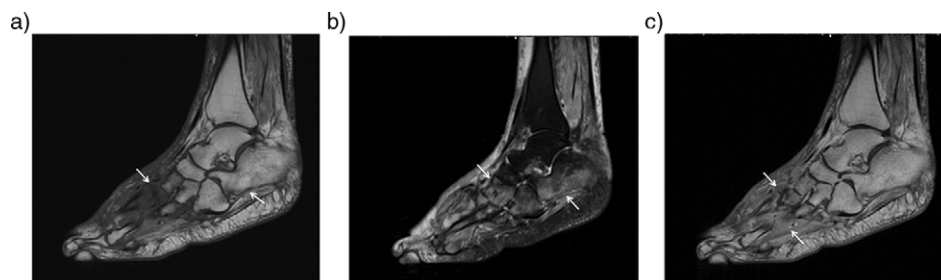


*Fig. 2.* Acute neuropathic arthropathy of the foot of 53-year-old woman with diabetes. Sagittal T1 (a) and T2-weighted fat saturated images (b) reveal diffuse bone marrow edema around the Lisfranc joint and calcaneus (arrows). There is also a subcutaneous soft tissue edema especially in the dorsum of the foot. Contrast enhanced sagittal T1-weighted image (c) shows increased enhancement in bone marrow and periarticular tissue (arrows). No evidence of fluid collection or sinus tract noted.
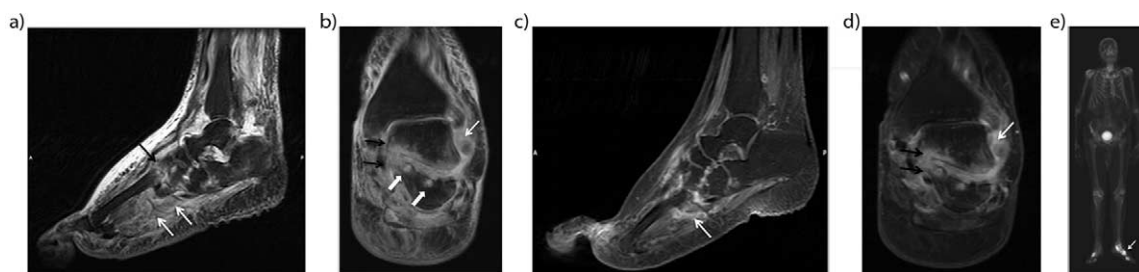
*Fig. 3.* Acute neuroarthropathy in an 80-year-old man with long-standing diabetes. Sagittal (a), and coronal (b) T2-weighted fat-saturated images demonstrated massive soft tissue edema in subcutaneous and periarticular region and periarticular bone marrow edema around the Lisfranc joints (black arrow) and posterior subtalar joint. Also note tiny cysts (solid white arrows) along the posterior subtalar joint. Sagittal (c) and coronal (d) post-contrast T1-weighted fat-saturated images demonstrated strong enhancement in the periartricular bone marrow (black arrows) and in the soft tissue planes (white arrows). Late phase bone scintigraphy (e) reveals an increased uptake along the affected bone and joints (arrow).

and bone marrow edema are not detected by PR. Plain radiography has low sensitivity and specificity rates (<50%) in detection of early findings of CN (9, 25, 26).

Traditionally, the evolution of diabetic neuroarthropathy of the foot has been discerned by radiography, according to Eichenholtz (27) into three different stages: bone dissolution (stage I), bone coalescence (stage II), and bone remodeling (stage III). Clinically, stages I and II are characterized by inflammatory edema of the foot, which is absent in stage III. This staging scheme is believed to represent the entire natural evolution of the condition, from the active inflamed stages to the healed, quiescent stage. However, the Eichenholtz classification does not include the stage preceding stage I which is clinically important (28, 29), and so-called stage 0 Charcot foot (30, 31). Stage 0 is characterized by inflammatory foot edema, like stage I and II. However, no radiographic bony abnormalities are present in this stage.

Since the early changes of neuroarthropathy such as bone marrow edema and microfractures cannot be distinguished in a CT examination, there is no potential role of CT in detecting early findings of acute CN (18, 32).

MRI, on the other hand, is the most sensitive modality in the detection of early changes of CN. On MR images of early stages of acute CN, there is a soft tissue edema. Furthermore, in the early stages of Lisfranc joint disease disruption of Lisfranc ligament could be detected with MRI that results in the malalignment and collapse of the longitudinal arch in early stages of the disease (33).

Soft tissue edemas, joint effusions, subchondral bone marrow edema of involved joints are the most commonly seen findings in acute CN (26, 34). Bone marrow edema is characterized by low signal intensity on T1-weighted, and high signal intensity on T2-weighted images. Extension of edema throughout medullary bone is possible (33). Bone-marrow enhancement is typically present predominantly in the subchondral region on gadolinium-enhanced studies (Figs. 2, 3) (31). Fractures related to neuropathic osteoarthropathy may also contribute to signal changes in the marrow and cortex that can lead to misinterpretation (35).

A variety of radionuclide studies have been used in CN. The technetium-99m methylene diphosphonate (Tc-MDP) bone scan is clinically useful in detecting and localizing abnormal bone, with high accuracy levels. In complicated cases in which there is an increased bone turnover (i.e. infection, trauma, surgery), specificity rates decreases. Reported sensitivity and specificity levels for the detection of osteomyelitis are 95–100% and 25–38%, respectively (36, 37). There is an increased uptake in all three (angiographic, blood pool, delayed), phases (Fig. 4), but same is true for osteomyelitis. A four-phased bone scan with delayed image acquisition at 24 hours, is more specific for detecting woven bone but conditions such as fractures,
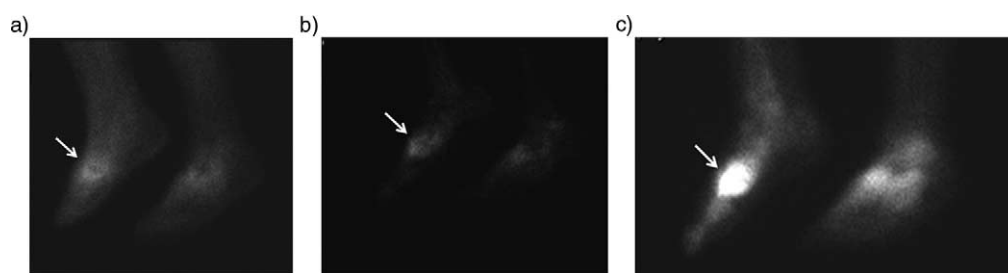


*Fig. 4.* Bone scan of a 53-year-old woman with a history of diabetes presented with swollen right with no skin ulcer. Three-phase (early, blood pool and delayed static phases) hydroxymethane diphosphonate (*99mTc-HDP*) bone scan demonstrated an increased uptake in all three phases, which is suggestive for diabetic neuroarthropathy (arrows).
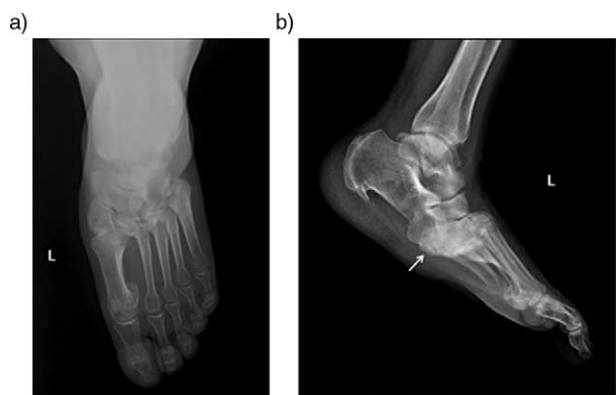
*Fig. 5.* Anteroposterior (a) and lateral (b) plain radiographs of the left foot in a diabetic patient with chronic neuropathic arthropathy in the midfoot affecting the Lisfranc joint. Note plantar subluxation of the hindfoot (arrow) with typical 'rocker-bottom' deformity and dorsal subluxation of metatarsal bases.

tumors and severe degenerative changes can also result in false-positive results (38).

Labelled white cell scans (In-WBC) do not usually accumulate at the sites of new bone formation without infection and are very useful for both diagnosis and follow-up of pedal osteomyelitis with an accuracy level of 80–90% (38). Therefore, a combination of three phase Tc-MDP and In-WBC scans, which has a sensitivity and specificity of 80–90%, is valuable for diagnosis if there is a penetrating ulcer underneath the deformity (38). However, in the presence of a recent onset, rapidly advancing CN, In-WBC scan can be falsely positive without any infection due to localization of labeled WBC at radiographically invisible periarticular microfractures (39).

The role of FDG-PET in the setting of diabetic neuro-osteoarthropathy has been assessed. Basu et al. (40) have found that FDG-PET is superior to MRI in the differentiation of CN from osteomyelitis in general and even in the presence of foot ulcers. Hopfner et al. also demonstrated a higher accuracy rate in the detection of osteomyelitis in patients with diabetic Charcot disease compared to MRI (41). Pickwell et al. (42) have compared the diagnostic power of bone scintigraphy and FDG-PET/CT in the diagnosis of acute CN, and found that FDG-PET/CT was better than the former. In FDG-PET/CT studies, increased uptake within soft tissues rather than bones is a commonly seen feature of CN. In a study carried out by Pickwell et al. (42), it has been stated that inflammation might be originated from soft tissues and than bones were consequently affected in the CN.

## Imaging of chronic stable CN

Clinically, a warm and red foot is no longer present in the chronic inactive stage. The edema may persist, but the difference in skin temperature between the feet is usually <2°C (23). Plain radiographs are valuable in the chronic stable CN (2, 5, 16, 38, 43) especially in follow-up of the patients. Chronic stage can be summarized with rule of "6 D's" that is representing joint distention, destruction, dislocation, disorganization, debris and increased bone density (9, 33). 'Pencil and cup' appearance in the forefoot secondary to metatarsophalangeal joint involvement can be seen. The involvement of tarsometatarsal (Lisfranc) joints lead to the collapse of the longitudinal arch, which results in increased load bearing on the cuboid and rocker-bottom deformity (Fig. 5). Talocalcaneal dislocation, talar collapse, atypical calcaneal fractures might be seen in hindfoot (9). Bone fragmentation and disorganization of affected joints and altered anatomy can be better evaluated with three dimensional and multiplanar reformatted CT images that might be helpful for surgical planning (18) (Fig. 6).

On MR images, edema and enhancement are less prominent or absent in the chronic form of neuropathic osteoarthropathy (33). Subchondral cysts appear as well-marginated foci of low signal intensity on T1-weighted
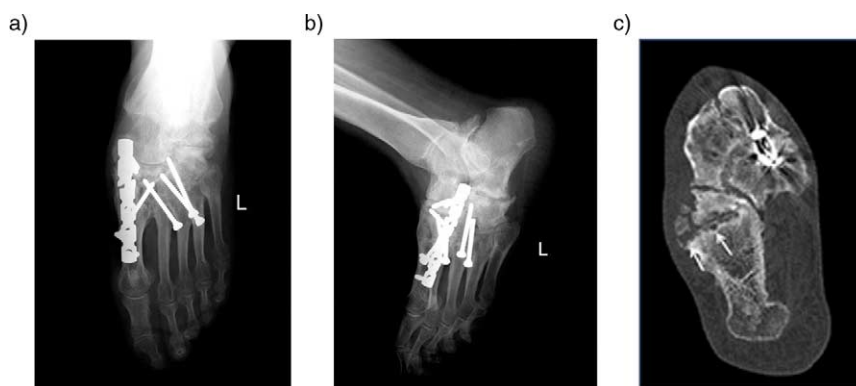


*Fig. 6.* Midfoot reconstruction in a 60-year-old patient with unstable neuropathic osteoarthropathy (a–c). Anteroposterior (a) and lateral (b) plain radiographs demonstrated neuropathic changes in midfoot region and complex realignment and fusion (a). Joint destruction osseous fragmentation and subchondral cyst formation (arrow) better delineated compared to PR in transverse CT image (c).
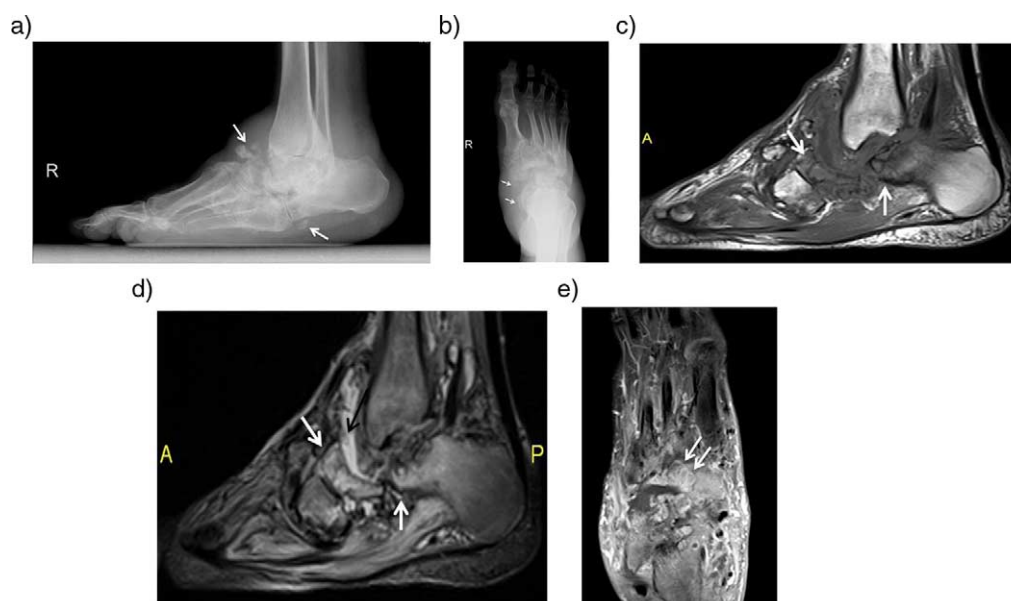
*Fig. 7.* Anteroposterior (a) and lateral (b) plain radiographs of the foot in a 57-year-old diabetic patient with longstanding neuropathic arthropathy show disorganization and fragments (white arrows) along Lisfranc and Chopart joints. Sagittal T1-weighted (c) and T2-weighted fat-saturated (d) images demonstrate periarticular bone marrow edema (white arrows), periarticular soft tissue collections (black arrow) in Chopart joint. Long-axis post-contrast T1-weighted image (e) reveals periarticular rim enhancing cyst formations (white arrows).

images and high signal intensity on T2-weighted images. Bone proliferation is present, with debris or intra-articular bodies (16) (Fig. 7). Typically, chronic neuropathic osteoarthropathy appears as decreased signal intensity, consistent with osteosclerosis on all sequences. Joint deformity, with subluxation or dislocation can be demonstrated with MRI (16, 44).

Superior and lateral subluxation of the metatarsals, and rocker bottom deformity due to the development of neuropathic disease of the Lisfranc joint may results in callus and ulcer formation beneath the cuboid and ulcers over the superiorly subluxed metatarsals (45) (Fig. 8).

## Differentiation of noninfected neuroartyhropathy from infected neuroarthropathy

Exclusion of concomitant infection in acute or subacute stage of CN is very challenging both clinically and radiologically. Both entities may present with symptoms such as swelling, redness, and tenderness. The presence of neuroarthropathy may limit the specificity of MR imaging for the detection of a superimposed infection. However, patients with neuroarthropathy and an ulcer that extends to the bone are more likely to also have osteomyelitis than patients with no preexisting neuroarthropathy.
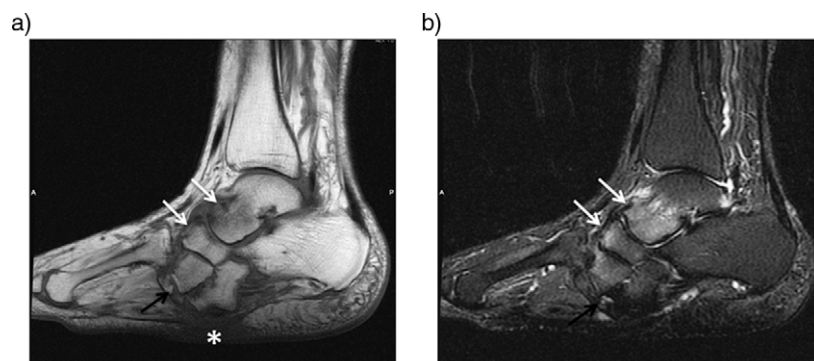


*Fig. 8.* Subacute neuroarthropathy of a 60-year-old woman. Sagittal T1-weighted (a) and T2-weighted fat-suppressed image (b) demonstrates rocker-bottom deformity. There is mild bone marrow edema in talonavicular and tarsometatarsal joints (white arrows) and bony fragments adjacent to lateral cuneiform (black arrows). Note the plantar skin callus beneath the cuboid due to altered biomechanics (asterisk).
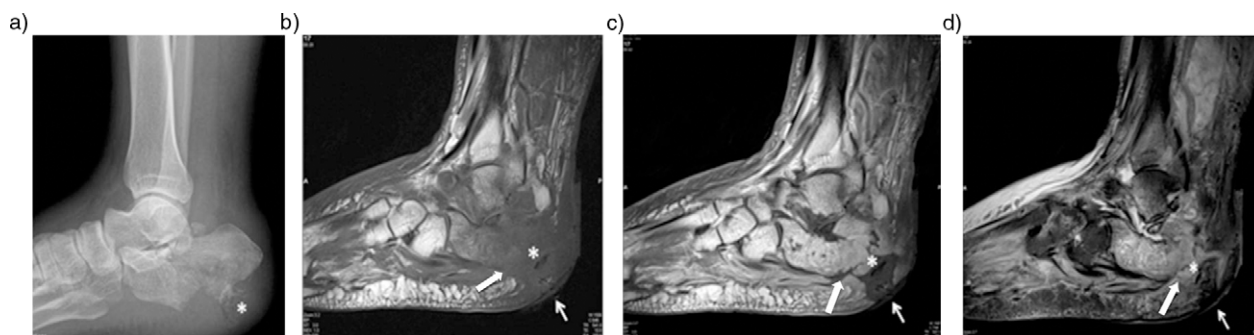
*Fig. 9.* A 57- year-old diabetic patient with longstanding neuropathic arthropathy. Plain radiograph shows hindfoot deformity and calcaneal fragmentation due to Charcot disease (a). T1-weighted sagittal pre (b) and post-contrast (c) and T2-weighted fat-suppressed (d) images reveal skin ulcer and associated a wide sinus tract formation (arrow) containing free air (asteriks), extending to bony cortex. Note the replacement of soft tissue fat (solid white arrow); subcutaneous and periarticular enhancement and osseous contrast enhancement that is consistent with infected neuroarthropathy.

Soft tissue findings of superimposed osteomyelitis are the absence of adjacent sub-cutaneous fat signal intensity and the presence of adjacent soft-tissue fluid collections that are larger than those typically seen in uninfected neuropathic joints, development of sinus tracts and ulcers extending to bony cortex (Fig. 9). Disappearance of subchondral cysts and bone fragments on follow-up examinations are considered as findings of superimposed infection. Bone marrow changes including increased T2 signal intensity and enhancement within bone marrow beyond the articular surfaces, progressive bone resorbtion

and increased periarticular contrast enhancement are also the signs of superinfection (46, 47) (Table 1). Follow-up and serial imaging is helpful for the evaluation of such patients (33).

## Differentiation of acute neuroarthropathy from osteomyelitis

The sensitivity and specificity of MR imaging for diagnosing osteomyelitis exceeds 90% in the absence of neuropathic disease (48). But the differentiation of acute neuroarthropathy from acute osteomyelitis is one of the

*Table 1.* MRI findings in non-infected and infected neuroarthropathy

| MRI feature | Non-infected neuroarthropathy | Infected neuroarthropathy |
|---|---|---|
| Periarticular fluid collection | + | + + |
| Sinus tract/abscess formation | − | + |
| Soft tissue fluid collections | Small | Large |
| Adjacent subcutaneous fat signal | Normal | Absent |
| Soft tissue enhancement | Limited to juxtaarticular soft tissue | Extensive |
| Subchondral degenerative cysts/intraarticular bodies | + | Disappears on follow up |
| Bone marrow edema | Periarticular/subchondral | Extensive, throughout the medullary bone |
| Bony cortex | Preserved | Erosion |
| 'Ghost sign'* | − | + |

*Reference 50. Refers to poor definition of the margins of a bone on T1-weighted images, that become clear after contrast administration.

*Table 2.* MRI findings in osteomyelitis and non-infected neuroarthropathy

| MRI feature | Osteomyelitis | Neuroarthropathy |
|---|---|---|
| Location | Phalanges, metatarsal heads, calcaneus, malleolus | Predominantly midfoot (tarsometatarsal, metatarsophalangeal joints) |
| Distribution | Focal involvement | Several joints/bones involved |
| Bone marrow signal changes | Around ulcers, fistula tracts, | Periarticular |
| Adjacent subcutaneous fat signal | Inflamed, sinus tracts, abscess formation | Edematous |
| Deformity | Usually not seen | Midfoot collapse |

most challenging issues in the evaluation of diabetes-related foot complications.

There are some features to help in distinguishing neuropathic arthropathy from osteomyelitis (Table 2). Marrow replacement with a low signal intensity on T1-weighted images and corresponding high signal intensity on T2-weighted images is characteristic for osteomyelitis, with or without notable cortical disruption (49). Although T2 hyperintensity is highly sensitive for osteomyelitis, if there is no corresponding low signal intensity on T1-weighted sequences, it might be representing osteitis secondary to adjacent soft tissue inflammation rather than osteomyelitis with medullary involvement. These signal changes should be carefully interpreted especially if there is no adjacent ulcer and presence of underlying neuropathic disease (50).

One of the most useful distinguishing feature of osteomyelitis is its location. Osteomyelitis develops almost exclusively by the contiguous spread of infection from skin ulcerations and sinus tracts, whereas neuropathic arthropathy is primarily periarticular (45). The presence of a bone marrow abnormality in the periarticular region without an adjacent ulceration is indicative of neuroarthropathy. Neuroarthropathy most commonly affects the tarsometatarsal and metatarsophalangeal joints, whereas osteomyelitis occurs distal to the tarsometatarsal joints in the calcaneus and malleolus and phalanges (50). Neuropathic arthropathy tends to involve several joints in a region, whereas infection tends to remain localized or spread contiguously (33).

## Summary

Diabetic CN is a chronic and progressive disease of bone and joints, characterized by painful or painless bone and joint destruction on limbs that have lost sensory innervation. Clinical diagnosis of CN is very challenging and MRI has an integral role to play in the radiological diagnosis of CN and associated infectious conditions.

## Conflict of interest and funding

## References

1. Charcot J. Sur quelques arthropathies qui paraissent dependre d'une lesion du cerveau ou de la moelle epiniere. Arch Des Phys Norm Pathol 1868; 1: 161.
2. Gouveri E, Papanas N. Charcot osteoarthropathy in diabetes: a brief review with an emphasis on clinical practice. World J Diabetes 2011; 2: 59–65.
3. Malhotra S, Bello E, Kominsky S. Diabetic foot ulcerations: biomechanics, charcot foot, and total contact cast. Semin Vasc Surg 2012; 25: 66–9.
4. Mumoli N, Camaiti A. Charcot foot. CMAJ 2012; 184: 1392.
5. Rogers LC, Frykberg RG, Armstrong DG, Boulton AJ, Edmonds M, Van GH, et al. The Charcot foot in diabetes. Diabetes Care 2011; 34: 2123–9.
6. Sanders LJ. The Charcot foot: historical perspective 1827–2003. Diabetes Metab Res Rev 2004; 20(Suppl 1): S4–8.
7. Petrova NL, Foster AV, Edmonds ME. Difference in presentation of charcot osteoarthropathy in type 1 compared with type 2 diabetes. Diabetes Care 2004; 27: 1235–6.
8. Chisholm KA, Gilchrist JM. The Charcot joint: a modern neurologic perspective. J Clin Neuromuscul Dis 2011; 13: 1–13.
9. Rajbhandari SM, Jenkins RC, Davies C, Tesfaye S. Charcot neuroarthropathy in diabetes mellitus. Diabetologia 2002; 45: 1085–96.
10. Armstrong DG, Todd WF, Lavery LA, Harkless LB, Bushman TR. The natural history of acute Charcot's arthropathy in a diabetic foot specialty clinic. Diabet Med 1997; 14: 357–63.
11. Clohisy DR, Thompson RC Jr. Fractures associated with neuropathic arthropathy in adults who have juvenile-onset diabetes. J Bone Joint Surg Am 1988; 70: 1192–200.
12. Bayne O, Lu EJ. Diabetic Charcot's arthropathy of the wrist. Case report and literature review. Clin Orthop Relat Res 1998; 357: 122–6.
13. Lambert AP, Close CF. Charcot neuroarthropathy of the knee in type 1 diabetes: treatment with total knee arthroplasty. Diabet Med 2002; 19: 338–41.
14. Petrova NL, Moniz C, Elias DA, Buxton-Thomas M, Bates M, Edmonds ME. Is there a systemic inflammatory response in the acute charcot foot? Diabetes Care 2007; 30: 997–8.
15. Sanders L, Frykberg R. Diabetic neuropathic osteoarthropathy: the Charcot foot. In: Frykberg R, ed. The high risk foot in diabetes mellitus. New York: Churchill Livingstone; 1991, pp. 297–338.
16. Sella EJ, Barrette C. Staging of Charcot neuroarthropathy along the medial column of the foot in the diabetic patient. J Foot Ankle Surg 1999; 38: 34–40.
17. Brodsky JW, Rouse AM. Exostectomy for symptomatic bony prominences in diabetic charcot feet. Clin Orthop Relat Res 1993; 296: 21–6.
18. Loredo R, Rahal A, Garcia G, Metter D. Imaging of the diabetic foot diagnostic dilemmas. Foot Ankle Spec 2010; 3: 249–64.
19. Loredo RA, Garcia G, Chhaya S. Medical imaging of the diabetic foot. Clin Podiatr Med Surg 2007; 24: 397–424.
20. Caputo GM, Ulbrecht J, Cavanagh PR, Juliano P. The Charcot foot in diabetes: six key points. Am Fam Physician 1998; 57: 2705–10.
21. Jeffcoate W, Lima J, Nobrega L. The Charcot foot. Diabet Med 2000; 17: 253–8.
22. Clouse ME, Gramm HF, Legg M, Flood T. Diabetic osteoarthropathy. Clinical and roentgenographic observations in 90 cases. Am J Roentgenol Radium Ther Nucl Med 1974; 121: 22–34.
23. Schoots IG, Slim FJ, Busch-Westbroek TE, Maas M. Neuroosteoarthropathy of the foot-radiologist: friend or foe? Semin Musculoskelet Radiol 2010; 14: 365–76.
24. Toledano TR, Fatone EA, Weis A, Cotten A, Beltran J. MRI evaluation of bone marrow changes in the diabetic foot: a practical approach. Semin Musculoskelet Radiol 2011; 15: 257–68.
25. Chantelau E, Poll LW. Evaluation of the diabetic charcot foot by MR imaging or plain radiography – an observational study. Exp Clin Endocrinol Diabetes 2006; 114: 428–31.
26. Morrison WB, Ledermann HP. Work-up of the diabetic foot. Radiol Clin North Am 2002; 40: 1171–92.
27. Eichenholtz SN. Charcot joints. Springfield, Illinois: Charles C Thomas; 1966, pp. 7–8.

28. Chantelau E. The perils of procrastination: effects of early vs. delayed detection and treatment of incipient Charcot fracture. Diabet Med 2005; 22: 1707–12.

29. Pakarinen TK, Laine HJ, Honkonen SE, Peltonen J, Oksala H, Lahtela J. Charcot arthropathy of the diabetic foot. Current concepts and review of 36 cases. Scand J Surg 2002; 91: 195–201.

30. Yu GV, Hudson JR. Evaluation and treatment of stage 0 Charcot's neuroarthropathy of the foot and ankle. J Am Podiatr Med Assoc 2002; 92: 210–20.

31. Yu JS. Diabetic foot and neuroarthropathy: magnetic resonance imaging evaluation. Top Magn Reson Imaging 1998; 9: 295–310.

32. Sartoris DJ. Cross-sectional imaging of the diabetic foot. J Foot Ankle Surg 1994; 33: 531–45.

33. Ledermann HP, Morrison WB. Differential diagnosis of pedal osteomyelitis and diabetic neuroarthropathy: MR imaging. Semin Msculoskelet Radiol 2005; 9: 272–83.

34. Marcus CD, Ladam-Marcus VJ, Leone J, Malgrange D, Bonnet-Gausserand FM, Menanteau BP. MR imaging of osteomyelitis and neuropathic osteoarthropathy in the feet of diabetics. Radiographics 1996; 16: 1337–48.

35. Moore TE, Yuh WT, Kathol MH, el-Khoury GY, Corson JD. Abnormalities of the foot in patients with diabetes mellitus: findings on MR imaging. AJR Am J Roentgenol 1991; 157: 813–6.

36. Schauwecker DS. The scintigraphic diagnosis of osteomyelitis. AJR Am J Roentgenol 1992; 158: 9–18.

37. Keenan AM, Tindel NL, Alavi A. Diagnosis of pedal osteomyelitis in diabetic patients using current scintigraphic techniques. Arch Intern Med 1989; 149: 2262–6.

38. Tomas MB, Patel M, Marwin SE, Palestro CJ. The diabetic foot. Br J Radiolol 2000; 73: 443–50.

39. Palestro CJ, Mehta HH, Patel M, Freeman SJ, Harrington WN, Tomas MB, et al. Marrow versus infection in the Charcot joint: indium-111 leukocyte and technetium-99m sulfur colloid scintigraphy. J Nucl Med 1998; 39: 346–50.

40. Basu S, Zhuang H, Alavi A. Imaging of lower extremity artery atherosclerosis in diabetic foot: FDG-PET imaging and histopathological correlates. Clin Nucl Med 2007; 32: 567–8.

41. Hopfner S, Krolak C, Kessler S, Tiling R, Brinkbaumer K, Hahn K, et al. Preoperative imaging of Charcot neuroarthropathy in diabetic patients: comparison of ring PET, hybrid PET, and magnetic resonance imaging. Foot Ankle Int 2004; 25: 890–5.

42. Pickwell KM, van Kroonenburgh MJ, Weijers RE, van Hirtum PV, Huijberts MS, Schaper NC. F-18 FDG PET/CT scanning in Charcot disease: a brief report. Clin Nucl Med 2011; 36: 8–10.

43. Ranachowska C, Lass P, Korzon-Burakowska A, Dobosz M. Diagnostic imaging of the diabetic foot. Nucl Med Rev Cent East Eur 2010; 13: 18–22.

44. Cofield RH, Morrison MJ, Beabout JW. Diabetic neuroarthropathy in the foot: patient characteristics and patterns of radiographic change. Foot Ankle 1983; 4: 15–22.

45. Ledermann HP, Morrison WB, Schweitzer ME, Raikin SM. Tendon involvement in pedal infection: MR analysis of frequency, distribution, and spread of infection. AJR Am J Roentgenol 2002; 179: 939–47.

46. Ahmadi ME, Morrison WB, Carrino JA, Schweitzer ME, Raikin SM, Ledermann HP. Neuropathic arthropathy of the foot with and without superimposed osteomyelitis: MR imaging characteristics. Radiology 2006; 238: 622–31.

47. Donovan A, Schweitzer ME. Use of MR imaging in diagnosing diabetes-related pedal osteomyelitis. Radiographics 2010; 30: 723–36.

48. Kapoor A, Page S, Lavalley M, Gale DR, Felson DT. Magnetic resonance imaging tor diagnosing foot osteomyelitis: a metaanalysis. Arch Intern Med 2007; 167: 125–32.

49. Morrison WB, Schweitzer ME, Bock GW, Mitchell DG, Hume EL, Pathria MN, et al. Diagnosis of osteomyelitis: utility of fatsuppressed contrast-enhanced MR imaging. Radiology 1993; 189: 251–7.

50. Donovan A, Schweitzer ME. Current concepts in imaging diabetic pedal osteomyelitis. Radiol Clin North Am 2008; 46: 1105–24.

*Saziye Eser Sanverdi
Birlik Mah. 462.sok. 5/6 06550
Ankara, Turkey
Tel: 0090 3124952885
Email: esersanverdi@yahoo.com